Signal Distortion Analysis of L-Shaped UWB Antenna

Eun-young Jung, Jae W. Lee, *Member, IEEE*, and Choon Sik Cho, *Member, IEEE*

***Abstract*—A printed L-shaped monopole antenna for applications in ultrawideband (UWB) systems such as home networks and various wireless systems is presented with signal transfer analyses both in the time and frequency domains. A miniaturization of the proposed antenna has been accomplished by folding and tuning the printed monopole antenna and considering the easy-mountable structure in high-data-rate wireless systems and universal serial bus (USB) dongle peripherals. The results obtained show that the input impedance bandwidth is approximately 6.6 GHz ranging from 4 to 10.6 GHz under the general criterion of VSWR less than 2:1. In addition, the relationship between the efficiency of data transfer and input/output signals is considered.**

***Index Terms*—Fidelity, L-shaped ultrawideband (UWB) antenna, signal distortion, transfer function.**

I. Introduction

RECENTLY, an increase in data rates and an improvement in data speed have been required for many services associated with the spread of wireless communication systems. As a candidate for satisfying these requirements and replacing the existing wireless standards, an ultrawideband (UWB) system with a millimeter-wave system has been suggested as a competitive service. In the extensive literature dealing with many different types of antenna for UWB systems [1], [2], much effort has been focused on the relationship between time- and frequency- domain characteristics using transmitting and receiving antennas.

Particularly, signal distortion in the time domain has been considered interesting by many researchers because of wideband occupancy, nonexistence of carrier frequencies, and narrowband interferences with already serviced frequencies such as WLAN and Bluetooth PANs [3]–[5].

There are many electrical goals for signal transfer from transmitting to receiving antennas without distortion. Hence, in this letter, return loss characteristics, radiation patterns, and the flatness of transfer functions between input and output signals have been investigated in the frequency domain, while the signal fidelity describing the relationship between input and output signals has been treated with various power distributions within the UWB frequency bands.

Manuscript received December 24, 2009; revised March 03, 2010 and May 31, 2010; accepted July 06, 2010. Date of publication July 19, 2010; date of current version August 16, 2010.

The authors are with the School of Electronics, Telecommunication and Computer Engineering, Korea Aerospace University, Gyeonggi 412-791, Korea (e-mail: jwlee1@kau.ac.kr).

Color versions of one or more of the figures in this letter are available online at http://ieeexplore.ieee.org.

Digital Object Identifier 10.1109/LAWP.2010.2058991

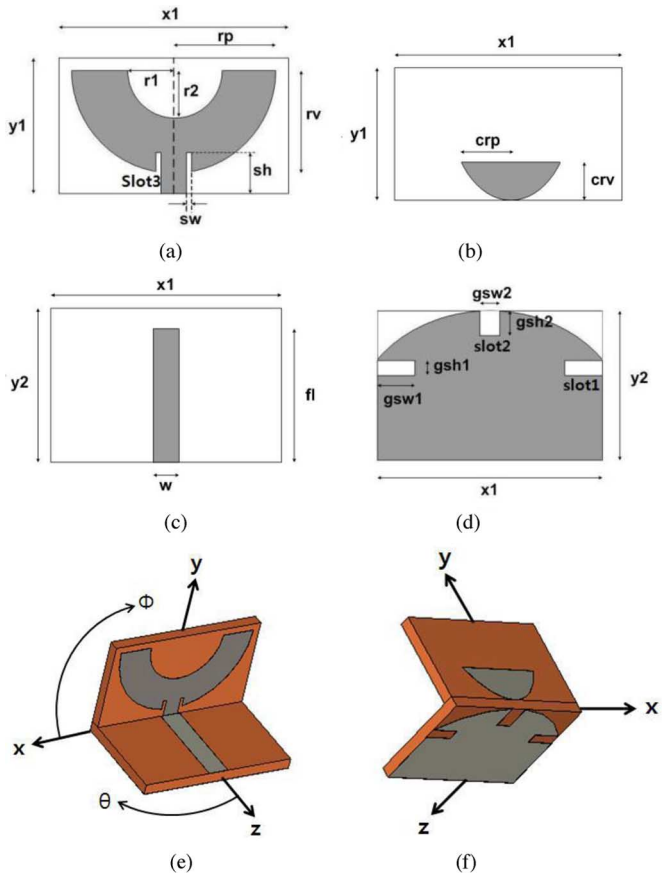

Fig. 1. Proposed L-shaped UWB antenna. (a) Inside view and (b) outside view in xy plane. (c) Inside view and (d) outside view in zx plane. (e), (f) Perspective view.

II. Antenna Design and Electrical Performance

Consider the proposed L-shaped monopole UWB antenna consisting of two orthogonal planes with the proper etched patterns as shown in Fig. 1.

By taking the size-reduction effects into account, the design of a planar-typed UWB antenna occupying an area of 24×29 mm^2, the optimized parameters of a nonplanar-type UWB antenna with an area of 24×15 mm^2 have been obtained and listed in Table I. Fig. 2 shows the simulated (CST MWS-based on a finite-difference time domain (FDTD) algorithm) and measured (measurements in the laboratory) return losses obtained by carrying out full electromagnetic (EM) simulations. In order to improve the reflection, several slots (numbered as slot 1, 2, and 3) have been used.

Fig. 2(a) shows that slot1 is very effective in generating a resonance frequency within 6–8 GHz, which is determined by the

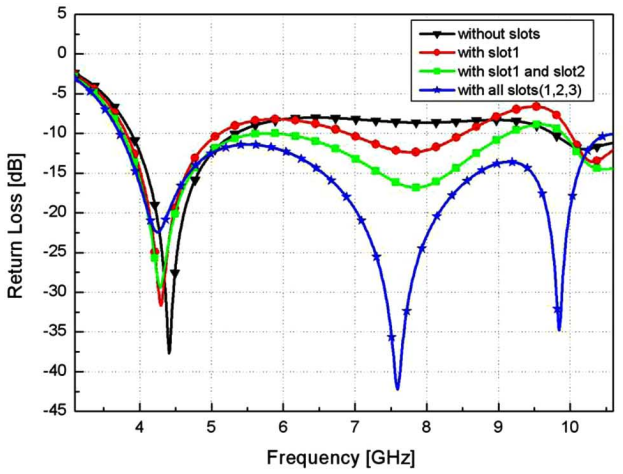

(a)

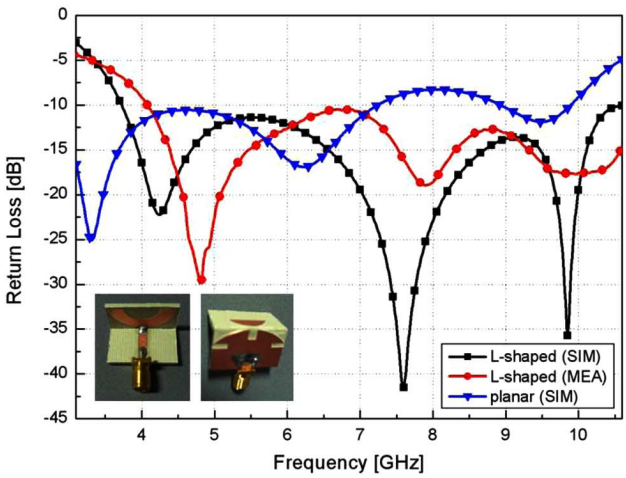

(b)

Fig. 2. Return losses versus frequency. (a) Reflection characteristics with various structures. (b) Measured and simulated results of the proposed and conventional antennas.

TABLE I
DESIGN PARAMETER VALUES FOR THE PROPOSED ANTENNA

parameter	value (mm)	parameter	value (mm)
x1	24	Sw	0.5
y1	13	Sh	2.5
y2	15	gsw1	4.5
rp	11	gsw2	2.5
rv	11	gsh1	1.5
r1, r2	6	gsh2	3.5
crp	6.8	W	3.1
crv	5	Fl	13.445

simple formula $\lambda_{\text{eff}}/4$. At this point, λ_{eff} and ε_{eff} are defined as $\lambda_{\text{eff}} = c/f\sqrt{\varepsilon_{\text{eff}}}$ and $\varepsilon_{\text{eff}} \simeq (\varepsilon_r + 1)/2$, respectively. At this time, the employed substrate has a relative dielectric constant of 3.5 and thickness of 1.52 mm. For further tuning of the resonant frequency, commercially available software has been employed for a parameter sweep operation. Fig. 2(b) shows the final reflection characteristics of the optimized L-shaped nonplanar UWB

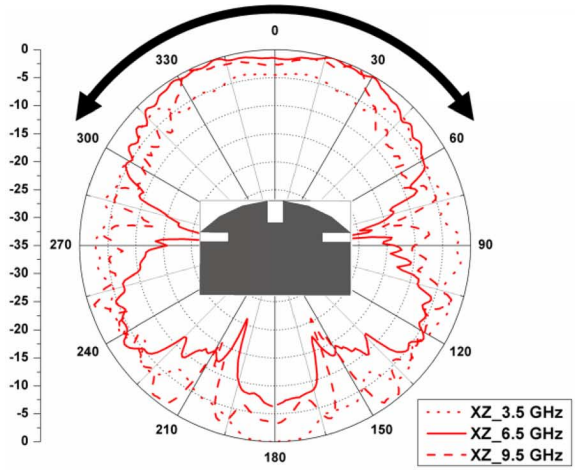

(a)

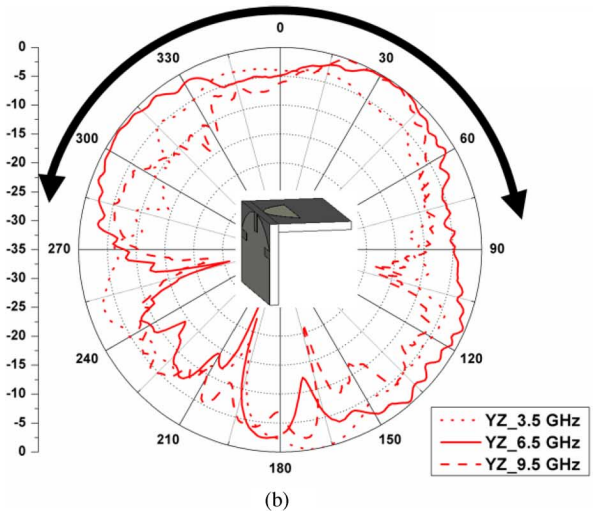

(b)

Fig. 3. Measured radiation patterns at three frequencies in two cutting planes. (a) xz plane. (b) yz plane.

antenna with that of a planar-type UWB antenna for a comparison of electrical performance. The main reason for the discrepancies between measured and simulated results in Fig. 2(b) is thought to be the effects of the variations in feeding microstrip widths in the manufacturing process on the resonance level near the resonant frequency.

Among many goals in antenna design, the main goal in radiation patterns of this letter is to achieve an omnidirectional radiation pattern within the arrow-indicating ranges in each plane of Fig. 3(a) and (b). From Fig. 3(a) and (b), it is ensured that the radiation patterns at three frequencies in the two cutting planes of the xz and yz planes are nearly omnidirectional patterns within the specified ranges suitable for wireless USB dongle devices.

III. SIGNAL TRANSFER ANALYSIS

A. Time Domain

In order to minimize the interferences caused by the UWB system, the Federal Communications Commission (FCC) has specified the emission mask of UWB signals in indoor/outdoor propagation by limiting the maximum emission levels to -41.3 dBm. In general, there are many signal waveforms that

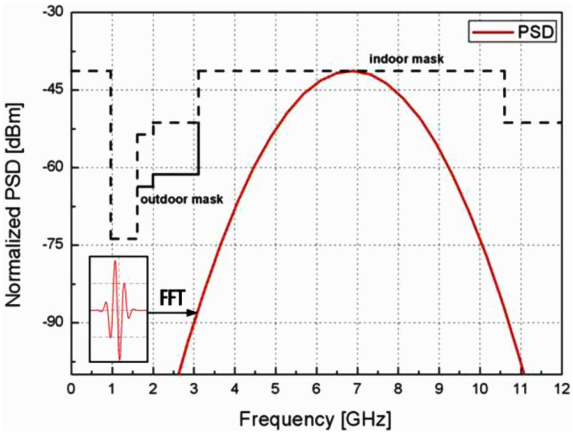

Fig. 4. Signal differentiated Gaussian pulse and spectral distribution in frequency domain.

TABLE II
FIDELITY OF SIGNAL IN TIME DOMAIN ACCORDING TO EQUATION (2)

Probe 1 ~ 5 (θ=270°) Probe 6 ~ 10 (θ=180°)	Fidelity							
	Case 1 : using 3.1 ~ 10.6 GHz)		Case 2 : using 4 ~ 10 (GHz)		Case 3 : using 5 ~ 9 (GHz)		Case 4 : using 6 ~ 8 (GHz)	
	S_{f_oo1}	S_{f_io1}	S_{f_oo2}	S_{f_io2}	S_{f_oo3}	S_{f_io3}	S_{f_oo4}	S_{f_io4}
Probe 1 (Φ=60°)	1	0.84	0.99	0.83	0.95	0.84	0.82	0.78
Probe 2 (Φ=30°)	1	0.88	0.99	0.88	0.97	0.87	0.86	0.79
Probe 3 (Φ=0°)	1	0.92	0.99	0.92	0.97	0.91	0.81	0.77
Probe 4 (Φ=−30°)	1	0.91	0.99	0.90	0.96	0.89	0.83	0.80
Probe 5 (Φ=−60°)	1	0.85	0.99	0.84	0.98	0.85	0.89	0.79
Probe 6 (Φ=60°)	1	0.97	0.99	0.96	0.99	0.94	0.88	0.82
Probe 7 (Φ=30°)	1	0.93	0.99	0.93	0.94	0.91	0.78	0.81
Probe 8 (Φ=0°)	1	0.87	0.99	0.87	0.96	0.86	0.84	0.78
Probe 9 (Φ=−30°)	1	0.90	0.99	0.90	0.94	0.89	0.81	0.79
Probe 10 (Φ=−60°)	1	0.87	0.99	0.87	0.95	0.87	0.81	0.79

are being considered. Among them, the seventh differentiated Gaussian pulse [6] (1) has been adopted as an input signal satisfying the requirement of the emission mask depicted in Fig. 4

$$s_{\mathrm{i}}(t) = c\left(\frac{t^6}{\sqrt{2\pi}\sigma^{13}} - \frac{15t^4}{\sqrt{2\pi}\sigma^{11}} - \frac{45t^2}{\sqrt{2\pi}\sigma^{9}} - \frac{15}{\sqrt{2\pi}\sigma^{7}}\right) \times \exp\left(-\frac{t^2}{2\sigma^2}\right) \quad (1)$$

where c is the constant determining the amplitude of a given pulse, and σ is the value of t when $s_{\mathrm{i}}(t) = e^{-1}$.

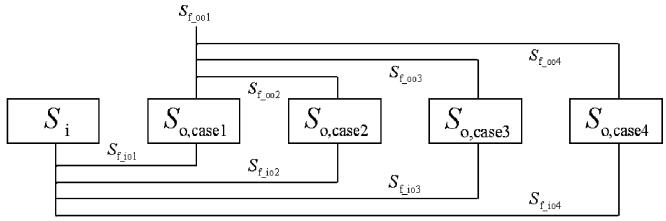

Fig. 5. Definitions of symbols described in Table II showing fidelity when S_i means the seventh differentiated Gaussian pulse as the input signal.

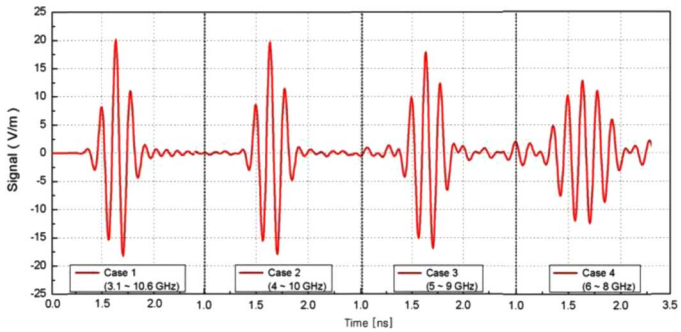

Fig. 6. Detected signals at the probe position with $\theta = 180°$ and $\phi = 60°$ in each case.

The UWB band has been divided into several cases according to the selected frequency range. Based on the similarity between input signal and detected signal at the probe position, the signal fidelity S_{f} describing the signal duplication has been obtained from (2) defined in [7]

$$S_{\mathrm{f}} = \max_{\tau} \frac{\int_{-\infty}^{\infty} s_{\mathrm{i}}(t)dt \int_{-\infty}^{\infty} s_{\mathrm{o}}(t-\tau)dt}{\sqrt{\int_{-\infty}^{\infty} s_{\mathrm{i}}^2(t)dt}\sqrt{\int_{-\infty}^{\infty} s_{\mathrm{o}}^2(t)dt}}. \quad (2)$$

In general, the similarity or fidelity between transmitted and received signals can be estimated as shown in Table II by using a correlation of the waveforms in the time domain since the information contained in transmitted and received signals in the frequency domain includes only the variation of magnitude in spectral distribution and renders clearly describing the amount of signal distribution or similarity difficult. The data in the second column $(S_{\mathrm{f\_ioj}})$ in each case listed in Table II assures that the fidelities ($S_{\mathrm{f\_io2}}$ and $S_{\mathrm{f\_io3}}$) of Cases 2 and 3 are nearly the same as that $(S_{\mathrm{f\_io1}})$ of Case 1 using the entire UWB frequency band as a reference within a 3% tolerance, whereas the differences between the fidelities ($S_{\mathrm{f\_io4}}$ and $S_{\mathrm{f\_io1}}$) of Cases 4 and 1 vary approximately from a minimum of 5% to a maximum of 16%. The symbol $S_{\mathrm{f\_ioj}}$ (or $S_{\mathrm{f\_ooj}}$) depicted in Fig. 5 represents the signal fidelity between the probed output signal at the jth case and the input signal S_i (or the probed output signal at Case 1) as a reference. Moreover, based on the data and analysis listed in Table II and Fig. 5, it can be conjectured that the probed signals with relatively wide bandwidth around the center frequency such as Cases 2 and 3 are useful for transmission without distortion as shown in Fig. 6, describing the similarities in waveforms between the detected signals at the probe position in Cases 1–4.

TABLE III
FLATNESS OF TRANSFER FUNCTION IN FREQUENCY DOMAIN ACCORDING TO EQUATION (3)

Probe 1 ~ 5 (θ=270°) Probe 6 ~ 10 (θ=180°)	3.1 ~ 10.6 (GHz) Case 1	5 ~ 9 (GHz) Case 3	6 ~ 8 (GHz) Case 4
Probe 1 (Φ=60°)	9.3428	6.8691	4.3020
Probe 2 (Φ=30°)	5.0703	3.5282	2.5812
Probe 3 (Φ=0°)	3.6865	1.6877	0.8837
Probe 4 (Φ=−30°)	3.6827	3.9737	2.8085
Probe 5 (Φ=−60°)	8.2418	6.8960	4.2894
Probe 6 (Φ=60°)	8.2543	2.7287	0.9935
Probe 7 (Φ=30°)	9.4843	2.6813	1.1980
Probe 8 (Φ=0°)	4.6712	1.7007	0.7677
Probe 9 (Φ=−30°)	4.9860	4.6605	2.7514
Probe 10 (Φ=−60°)	11.4659	6.7086	3.7966

B. Frequency Domain

In general, the transfer function in UWB communication is defined as the ratio of the Fourier transform of output or detected signal $S_{\mathrm{o}}(f)$ at the probed position and the antenna input signal $S_{\mathrm{i}}(f)$ like (3) in [8]

$$\mathrm{T.F.} = H(r,\theta,\omega) = \frac{S_{\mathrm{o}}(r,\theta,\omega)}{S_{\mathrm{i}}(r,\theta,\omega)}. \tag{3}$$

With a definition of the transfer function, the flatness of the transfer function in a given frequency band has been evaluated from the fundamental formula using standard deviation. Table III describes the flatness of the transfer function according to cases dependent on the considered frequencies. As expected, the smaller the used frequency band, the better the value of flatness. However, it is noted that the optimum case should be determined from the time-domain data as well as frequency-domain data.

IV. CONCLUSION

The signal transfer characteristics using the designed L-shaped antenna with a seventh differentiated Gaussian pulse have been rigorously analyzed in both the time and frequency domains.

Based on the emphasis of distortion-free signal transfer in UWB communications, the fidelities between the input and the probed output signals according to position have been estimated using a correlation formula. As a result shown in time- and frequency-domain analysis, it may be recommended that the choice of an optimized antenna and input signal form should simultaneously depend on both fidelity and local flatness for signal transmission and reception with little distortion.

REFERENCES

[1] J.-P. Zhang, Y.-S. Xu, and W.-D. Wang, "Microstrip-fed semi-elliptical dipole antennas for ultrawideband communications," *IEEE Trans. Antennas Propag.*, vol. 56, no. 1, pp. 241–244, Jan. 2008.
[2] H. K. Kan, W. S. T. Rowe, and A. M. Abbosh, "Compact coplanar waveguide-fed ultra-wideband antenna," *Electron. Lett.*, vol. 43, pp. 654–656, Jun. 2007.
[3] F. Viani, L. Lizzi, R. Azaro, and A. Massa, "A miniaturized UWB antenna for wireless dongle devices," *IEEE Antenna Wireless Propag. Lett.*, vol. 7, pp. 714–717, 2008.
[4] J. W. Lee, C. S. Cho, and J. Kim, "A new vertical disc-loaded ultra-wideband monopole antenna (VHDMA) with a horizontally top-loaded small disc," *IEEE Antenna Wireless Propatg. Lett.*, vol. 4, pp. 198–201, 2005.
[5] D. Kim, J. W. Lee, C. S. Cho, and T. K. Lee, "Time-domain investigation of notched VHDMA for UWB communications," in *Proc. APMC*, Dec. 2007, pp. 11–14.
[6] Y. J. Cho, K. H. Kim, D. H. Choi, S. S. Lee, and S.-O. Park, "A miniature UWB planar monopole antenna with 5-GHz band-rejection filter and the time-domain characteristics," *IEEE Trans. Antennas Propag.*, vol. 54, no. 5, pp. 1453–1460, May 2006.
[7] O. E. Allen, D. A. Hill, and A. R. Ondrejka, "Time-domain antenna characterizations," *IEEE Trans. Electromagn. Compat.*, vol. 35, no. 3, pp. 339–346, Aug. 1993.
[8] T.-G. Ma and S.-K. Jeng, "Planar miniature tapered-slot-fed annular slot antennas for ultrawide-band radios," *IEEE Trans. Antennas Propag.*, vol. 53, no. 3, pp. 1194–1202, Mar. 2005.
[9] N. Telzhensky and Y. Leviantan, "Novel method of UWB antenna optimization for specified input signal forms by means of genetic algorithm," *IEEE Trans. Antennas Propag.*, vol. 54, no. 8, pp. 2216–2225, Aug. 2006.